promotor; internal ribosomal entry site (IRES) followed by *Venus*, which is a variant of GFP, an improved version of yellow fluorescent protein as described previously (27); and a woodchuck hepatitis virus posttranscriptional regulatory element (PRE). The luciferase gene fragment was excised from the pGL3-Basic vector (Promega, Madison, WI) and cloned into pCS II -EF-MCS-IRES2-Venus at the *Bam*H1 site (Fig. 1*A*). Twenty-four hours before transfection, 293T cells were seeded in poly-L-lysine-coated T175 flask. The cells were transfected using lipofection protocol of the FuGENE6 transfection reagent (Roche, Indianapolis, IN). Two days after transfection, the conditioned medium was collected and the virus was concentrated by centrifugation at 21,000 rpm for 2 h at 4°C. The pelleted virus was resuspended and stored frozen at –80°C. The titer of concentrated virus was 1×10^8 to 2×10^8 transducing units per milliliter (TU/ml) when assayed on 293T cells, and infectivity was determined by GFP expression as analyzed on FACS calibur (Becton-Dickinson, Franklin, Lakes, NJ).

NSPC primary cultures

The methods for the culture and expansion of NSPCs have been described previously (2). In brief, the striatum of C57BL/6J mouse on embryonic day 14 was dissociated using a fire-polished glass pipette, and the dissociated cells were then collected by centrifugation and resuspended in separate culture medium. The culture medium consists of DMEM/F12 supplemented with the hormone mixture as described previously (2), and human recombinant fibroblast growth factor-2 (FGF-2) and epidermal growth factor (EGF) (20 ng/ml each) were added every 2 days. The cells formed floating cell clusters (neurospheres) within 2–3 days. The concentrated viruses were added into the culture medium to infect primary NSPCs (multiplicity of infection, MOI=1.0). After being propagated with two passages, neurospheres were used for in vivo BLI or dissociated into single cells and plated onto poly-L-ornithine-coated cover slips at a density of 1×10^5 cells/ml for in vitro assay. Both the untreated NSPCs and virally transduced NSPCs were allowed to differentiate for 7 days and were fixed with 4% paraformaldehyde in 0.1 M phosphate-buffered saline (PBS) for immunohistochemistry.

SCI model

Adult female C57BL/6J mice (20–22 g) were anesthetized via an i.p. injection of ketamine (100 mg/kg) and xylazine (10 mg/kg). After laminectomy at the 10th thoracic spinal vertebrae (T10), the dorsal surface of dura matter was exposed and SCI was induced using a commercially available SCI device (IH impactor, Precision Systems and Instrumentation, Lexington, KY) as described previously (28). This device creates a reliable contusion injury by rapidly applying a force-defined impact (60 kdyn) with a stainless steel-tipped impounder. Motor function of the hind limbs was evaluated by the locomotor rating test on the Basso-Beattie-Bresnahan (BBB) scale as described previously (29, 30) until 6 wk after injury. All procedures were approved by the ethics committee of Keio University, which were in accordance with the Guide for the Care and Use of Laboratory Animals (National Institutes of Health, Bethesda, MD)

Transplantation

For in vivo BLI, transplantation of lentivirally transduced NSPCs was performed by using a glass micropipette and a stereotaxic injector (KDS 310, Muromachi-kikai, Tokyo, Japan). The tip of the micropipette was inserted into the epicenter of the injured spinal cord, and 2 μl of the suspension of NSPCs was injected at a rate of 0.5 μl/min. The number of viable cells in the

suspensions was determined by cell counting using Trypan blue dye exclusion, and cell density was adjusted to an approximate range of 1.25×10^7 to 2.5×10^8 cells/ml to examine the correlation between cell numbers and bioluminescent signal. To examine the survival rate of NSPCs in the injured spinal cord, we performed transplantation of NSPCs (5×10^5) immediately after injury (acute transplantation, n=8) or at 9 days after injury (delayed transplantation, n=8). Instead of NSPCs, the culture medium without growth factors was injected into the lesion site at 9 days after injury in the control group (n=8).

Immunohistochemistry

Animals were anesthetized and transcardially perfused with 4% paraformaldehyde in 0.1 M PBS at 6 wk after injury. The spinal cords were removed, embedded in OCT compound, and sagittally sectioned at 20 μm on a cryostat. Both cultured cells and tissue sections were stained with primary antibodies, including anti-GFP (1:500; MBL, Woburn, MA), anti-Nestin (1:200; Chemicon, Temecula, CA), anti-luciferase (1:100; Rockland Immunochemicals, Gilbertsville, PA), anti-glial fibrillary acid protein (GFAP) (1:1000; DAKO, Glostrup, Denmark), anti-βIIItubulin (Tuj-1) (1:200; Sigma, St. Louis, MO), anti-APC CC-1 (1:200; Oncogene, Cambridge, MA), anti-2',3'-cyclic nucleotide 3'-phosphodiesterase (CNPase) (1:200; Sigma), and anti-Hu (a gift from Dr. Robert Darnell, The Rockefeller University). Nuclear counterstaining was obtained with Hoechst 33342 (Molecular Probes, Eugene, OR). Images were obtained by fluorescence microscopy (Axioskop 2 plus; Carl Zeiss, Munich, Germany) or confocal microscopy (LSM510; Carl Zeiss). To quantify the proportion of each phenotype in vivo, we selected five representative midsagittal sections and captured five regions within 500 μm rostral and caudal to the lesion epicenter randomly at ×200 magnification. GFP-positive engrafted cells as well as each phenotypic marker-positive cells were counted in each section.

BLI

Xenogen-IVIS 100 cooled CCD optical macroscopic imaging system (SC BioScience, Tokyo, Japan) (31) was used for BLI. Signal intensity of NSPCs was determined by plating cells at various densities and imaging immediately after D-luciferin (150 μg/ml) was added. Signals are reported as photons/cell/s. The integration time was fixed at 5 min duration for each image. For in vivo imaging, mice were given an i.p. injection of D-luciferin (150 mg/kg body weight), and serial images were acquired from 15–40 min after the administration until the maximum intensity was obtained with the field-of-view set at 7.2 cm. We found this time window to be optimal since the signal intensity peaked at 15 min after administration followed by a plateau of 20 min (data not shown). All images were analyzed with Igor (WaveMetrics, Lake Oswego, OR) and Living Image software (Xenogen, Alameda, CA), and optical signal intensity was expressed as photon flux, in units of photons/s/cm^2/steradian. Each image was displayed as a false color photon count image superimposed on a grayscale anatomic image. To quantify the measured light, we defined regions of interest (ROI) over the cell-implanted area and examined all values with the same ROI.

Statistical analysis

Statistical analysis was performed with a Student's t test. For the open field score, repeated measure ANOVA, Kruskal-Wallis test, and post hoc Bonferroni/Dunn test were used. Values are reported as mean ± SE. In all statistical analyses, significance was accepted at $P < 0.05$.

RESULTS

Imaging of lentivirally transduced NSPCs

NSPCs were harvested and labeled with luciferase and GFP reporter genes via lentiviral transduction. To examine the sensitivity of BLI, we used the CCD-based macroscopic detector to detect luminescence intensity of theses cells at various cell numbers (ranging from 10^2 to 10^6 cells per well) in the presence of D-luciferin (150 μg/ml). Quantitative analysis of bioluminescence revealed that luminescence intensity was clearly in direct proportion to cell numbers in vitro (Fig. 1*B*). A population of 100 cells was sufficient to produce a signal that was significantly above background.

Additionally, the intense luminescence of NSPCs enabled us to detect a single neurosphere with the CCD macroscope (Fig. 1*C–E*), and sufficient fluorescence and bioluminescence were detected from these cells with fluorescence microscopy (Fig. 1*F–H*). FACS calibur analysis revealed that >70% of these cells were positive for GFP (data not shown).

To confirm that lentiviral transduction had not altered the properties of NSPCs, we performed immunostaining and differentiation assays on labeled and untreated NSPCs. Fluorescence microscopy and immunostaining with anti-luciferase antibody confirmed the expression of luciferase and GFP in lentivirally transduced NSPCs (Fig. 2*A*, 2*B*). Both untreated and lentivirus-transfected NSPCs were allowed to differentiate for 7 days without growth factors in vitro. There were no differences in cell viability, in the pattern of phenotypes after differentiation, or in the ability to differentiate into neurons, astrocytes, and oligodendrocytes; some of them were positive for Nestin (32), a marker of NSPCs (Fig. 2*C–G*). Additionally, the stable expression of both luciferase and GFP in transduced NSPCs was maintained after differentiation (data not shown). These results demonstrated the ability of lentiviral vectors to confer high levels of specific gene expression while preserving the character of NSPCs.

In vivo imaging of transplanted cells

Since the signal from the labeled NSPCs appeared to be sufficient for in vivo cell tracking and viability studies, 5×10^5 of labeled NSPCs were stereotactically transplanted into the intact spinal cord of adult C57BL/6J mouse and cell distribution and signal intensity were assessed using BLI. On the exposed spinal cord, an intense focal spot of bioluminescence was observed at the transplanted site (Fig. 3*A*), indicating transplantation and placement of the cells into the spinal cord and not the surrounding tissue; this was confirmed by excising the spinal cord and observing its bioluminescence (Fig. 3*B*). To examine whether the number of the transplanted cells correlated with the intensity of bioluminescent signal in vivo, we performed transplants with different numbers of NSPCs (ranging from 25,000 to 500,000) at the level of T10 and assessed the signal intensity by BLI. The results indicated that the signal intensity was proportional to the number of transplanted cells; this was despite the use of mice with dark fur and skin, C57BL/6J (Fig. 3*C*, 3*D*), which had been believed inappropriate for optical imaging due to absorbance of the signals.

Viability of engrafted NSPCs in injured spinal cord

The great advantage of BLI is the capability to quantify only living cells since the luciferin-luciferase reaction depends on oxygen and ATP. To examine the engrafted cell viability in the injured spinal cord, we induced contusion injury at T10 level of adult mice and then transplanted 5×10^5 NSPCs in 2 μl medium at the lesion site. The accuracy of transplantation could be confirmed immediately after transplantation using BLI, and the average signal intensity was $4.60 \pm 0.45 \times 10^6$ photons/mouse/s in 16 mice. Images were obtained daily for 1 wk and then weekly over a 6-wk period. To investigate whether there is a relation between the timing of transplantation and grafted cell viability, we performed transplant operation either immediately (acute transplantation) or at 9 days after contusion injury (delayed transplantation). Analysis of both acute and delayed transplantation groups revealed drastic reductions in signal intensity within the first 4 days after transplantation, which was followed by a relatively stable bioluminescent signal for 6 wk (Fig. 4*A*). Quantitative comparison between the two groups revealed that there were no apparent differences in photon emission, suggesting that cell viability was comparable in acute and delayed transplantation (Fig. 4*B*, 4*C*). In mice that were not killed at the end of the experimental period, the bioluminescent signal could be followed for up to 10 months after transplantation in both groups (data not shown).

Integrated cell morphology in acute and delayed transplantation

Although no significant differences in cell viability were observed between the acute and delayed transplantation, there were apparent differences in the location and morphology of the integrated cells. SCI in C57BL/6J mice results in large connective tissue scars at the lesion epicenter dependent on the degree of crush injury (33) compared with cavity formation that is usually observed in the injured spinal cords of rats (29) or primates (34). The significant difference that was observed between the acute and delayed transplantation groups was that in the acute group NSPCs were mainly distributed within the scar area, while in the delayed group the NSPCs were found around the scar (Fig. 5*A* and 5*B*). Moreover, immunostaining and confocal microscopic images revealed that these integrated cells within the scar area of the acute group were GFAP-positive, and their morphology suggested that they contributed to the formation of an astrocytic glial scar (Fig. 5*C–E*, Supplemental Fig. 1). There was a small percentage of neurons (1.27%) and oligodendrocytes (0.99%) in the acute group (Table 1). In contrast, some of the grafted cells in the delayed group appeared to be single cells that expressed the oligodendrocyte marker APC (Fig. 5*F–H*), or the neuronal maker Hu (Fig. 5*I–K*, Supplemental Fig. 2) (Table 1). These results suggested that the microenvironment of injured spinal cord had a distinct influence on the differentiation of transplanted NSPCs.

Migratory cells were reflected in the configuration of bioluminescence

In the course of tracking luminescent signals of grafted NSPCs for 6 wk, the luminescent configuration changed from a round to an elliptic shape in mice of the delayed transplantation group (Fig. 6*A*). NSPCs transplanted into lesion epicenter (Fig. 6, *) migrated away caudally while extending the neurites, and there was a correspondence between histological and in vivo BLI (Fig. 6*B*). Migratory cells were mainly found along the white matter of the host spinal cord, and the confocal microscopic image revealed that some of these cells were Hu-positive neurons (Fig. 6*C–E*).

Transplanted NSPCs partially promoted functional recovery

The histological assays suggested that the timing of transplantation may also affect functional recovery. Here we used a standardized open-field measure of locomotor function: the BBB score to assess function in acute and delayed transplantation. In both treated groups, partial prompt recovery of hind-limb movement was observed within 1 wk after transplantation and was followed by a period of gradual recovery. While improved recovery was found in both acute and delayed transplantation groups compared with the medium-injected control group, the mice in the delayed transplantation group showed a tendency of long-lasting recovery, and the only statistically significant difference was between the control group and the delayed transplantation group with the post hoc Bonferroni/Dunn test (Fig. 7).

DISCUSSION

The present study is the first to use molecular imaging tools to monitor primary NSPCs and their accurate viability after transplantation into injured spinal cords in living animals. Although the feasibility and usefulness of in vivo BLI have been demonstrated in several studies, the conventional application of BLI was to track grafted cells whose signal intensity would increase with time, such as tumor cells or established cell lines, and long-term tracking of primary cultured NSPCs has been relatively difficult because unlike immortalized or proliferative cells, a large percentage of cells were lost within a short time period after transplantation. Furthermore, it has been difficult for primary cells to obtain high levels of sustained reporter gene expression compared with cell lines. To overcome this limitation and to follow primary cells in vivo, we used third-generation lentiviral vectors to transfer the luciferase and GFP genes to NSPCs. The transduction efficiency was high in the present study, owing to the ability to concentrate the vectors to high titers using their modified envelop glycoprotein from vesicular stomatitis virus (VSV-G). Their broad host range and their ability to infect nondividing cells and to integrate make these vectors ideal for gene transfer into NSPCs (24, 35). Transduced NSPCs demonstrated sustained expression of luciferase while maintaining the characteristic features of NSPCs (Fig. 2). Their bioluminescent signals appeared as a focal spot after transplantation into injured spinal cords of mice. By combining two novel tools, the third-generation lentiviral vectors and in vivo BLI, we could successfully monitor primary NSPCs transplanted into injured spinal cords, even with the dark skin of C57BL/6J mice, over long periods of time.

In the research of cell therapy, the accuracy of transplantation is a fundamental premise and especially significant when using small animals such as mice. Here we used BLI as a novel tool for confirming successful transplantation. The standard error of the mean in the signal value was $<10\%$ when 5×10^5 NSPCs were transplanted into injured spinal cords of 16 mice, which was an acceptable value for experimentation.

One of the advantages of BLI is to demonstrate the migration of grafted cells in living animals as Tang et al. (36) and Kim et al. (37) have previously reported. Here we demonstrate the stability of signals from NSPCs that integrated at the lesion epicenter in the acute transplantation group (Fig. 4*A*), and histology confirmed that the cells remained and participated in the formation of a glial scar at the scar area (Fig. 5*A*). In the delayed transplantation groups, NSPCs integrated around the scar area and differentiated into migrating neurons, and the images from BLI corresponded with the histological images (Fig. 6).

Signals in BLI have been shown to correlate with cell viability in a number of models (18, 23, 38). In the viability studies, we observed significant reductions in signal intensity over the first 4 days posttransplantation. This was followed by a period of relatively stable signal (6 wk), which was observed in both the acute and delayed transplantation groups (Fig. 5*A*). These data suggested that ~80% of NSPCs were lost within 4 days of transplantation and the remaining 15–20% of transplanted NSPCs survived over 6 wk (Fig. 5*C*). Several other studies have reported that few NSPCs integrated into the injured spinal cord and participated in the glial scar if transplanted at the time of acute injury (9, 39). Despite our expectation of a better survival rate in the delayed transplantation group, the results showed no apparent differences between the two groups. Histological examination confirmed the presence and integration of transplanted cells in both groups, with differences in location and differentiated cell type. Discrepancies between other previous reports (9) and the present study may be due to differences in the animals and models of SCI. In the contusive SCI of C57BL/6J mice, a large connective tissue scar typically forms at the lesion epicenter (33) and transplanted cells were mainly contained within this scar in this study. In contrast, in similar transplantation experiments in other animals, including rats and primates, large cavities are formed at the lesion epicenter that result in tissue necrosis, and the survival of cells transplanted into the lesion site in the acute phase was low.

Histological examination in our model revealed that the morphology of integrated cells was clearly different depending on the timing of transplantation (Fig. 5 and Table 1). These phenotypic differences may be due to differences in the microenvironment since the environment changes dramatically during this time. In the acute phase after injury, a transient and dramatic increase in chemical mediators and cytokines, for example, IL-1β, IL-6, CNTF, and TNF-α, are observed around the injured site (40), and they are likely to influence the differentiation of transplanted NSPCs. IL-6, CNTF, and BMPs induce NSPCs to undergo astrocytic differentiation selectively both in vivo and in vitro (30, 41, 42), and the majority of acutely transplanted NSPCs formed a glial scar at the lesion epicenter. NSPCs transplanted in the delayed phase appeared to differentiate into neurons and oligodendrocytes in addition to astrocytes (Table 1, Fig. 5 and 6).

We also evaluated the recovery of locomotor function for 6 wk and examined the correlation between the functional recovery and cell viability estimated by luminescent intensity. Better recovery was found in NSPC transplanted groups compared with the medium injected control group (Fig. 7), and significant differences were observed in motor function scores at 6 wk and signal intensity at 4 days or 6 wk, as the result of Spearman's correlation coefficient by rank test. The fact that there was no statistically significant difference between the acute and delayed transplantation groups with post hoc test suggests that the greatest contribution of NSPCs to functional recovery may be the secretion of neurotrophic factors (4, 43). However, considering that the only significant difference shown was between the control and delayed tranplantation groups, and that the delayed transplantation group showed a tendency of long-lasting recovery, the morphological difference revealed between the acute and delayed groups may be significant. Although additional studies will be needed to determine the precise mechanism of functional recovery by NSPC transplantation, delayed transplantation is considered to also be more practical from the aspect of clinical applications.

The methods in the present study can be widely applied to transplantation research and the study of primary cultured cells in the context of living animal models. Image guidance in this study offered the opportunity to monitor engraftment and migration, which were used to select the times for tissue sampling. Here, we used this approach to demonstrate the differences between

early and delayed cell transplantation, and the functional data suggest that delayed transplantation could have significant clinical efficacy.

ACKNOWLEDGMENTS

This work was supported by grants from the Japan Science and Technology Agency, Core Research for Evolutional Science and Technology, a Grant-in-Aid for the 21st century COE program, Keio Gijuku Academic Development Funds, National Grant-in-Aid for the Establishment of High-Tech Research Center, and the National Institutes of Health (R24 CA 92862 to CHC).

REFERENCES

1. Alvarez-Buylla, A., and Lim, D. A. (2004) For the long run: maintaining germinal niches in the adult brain. *Neuron* **41,** 683–686

2. Reynolds, B. A., Tetzlaff, W., and Weiss, S. (1992) A multipotent EGF-responsive striatal embryonic progenitor cell produces neurons and astrocytes. *J. Neurosci.* **12,** 4565–4574

3. Gage, F. H. (2000) Mammalian neural stem cells. *Science* **287,** 1433–1438

4. Okano, H. (2002) Stem cell biology of the central nervous system. *J. Neurosci. Res.* **69,** 698–707

5. Lindvall, O., Kokaia, Z., and Martinez-Serrano, A. (2004) Stem cell therapy for human neurodegenerative disorders-how to make it work. *Nat. Med.* **10, Suppl,** S42–S50

6. Bjorklund, A., Dunnett, S. B., Brundin, P., Stoessl, A. J., Freed, C. R., Breeze, R. E., Levivier, M., Peschanski, M., Studer, L., and Barker, R. (2003) Neural transplantation for the treatment of Parkinson's disease. *Lancet Neurol.* **2,** 437–445

7. Hallbergson, A. F., Gnatenco, C., and Peterson, D. A. (2003) Neurogenesis and brain injury: managing a renewable resource for repair. *J. Clin. Invest.* **112,** 1128–1133

8. Jeong, S. W., Chu, K., Jung, K. H., Kim, S. U., Kim, M., and Roh, J. K. (2003) Human neural stem cell transplantation promotes functional recovery in rats with experimental intracerebral hemorrhage. *Stroke* **34,** 2258–2263

9. Ogawa, Y., Sawamoto, K., Miyata, T., Miyao, S., Watanabe, M., Nakamura, M., Bregman, B. S., Koike, M., Uchiyama, Y., Toyama, Y., et al. (2002) Transplantation of in vitro-expanded fetal neural progenitor cells results in neurogenesis and functional recovery after spinal cord contusion injury in adult rats. *J. Neurosci. Res.* **69,** 925–933

10. Hofstetter, C. P., Holmstrom, N. A., Lilja, J. A., Schweinhardt, P., Hao, J., Spenger, C., Wiesenfeld-Hallin, Z., Kurpad, S. N., Frisen, J., and Olson, L. (2005) Allodynia limits the usefulness of intraspinal neural stem cell grafts; directed differentiation improves outcome. *Nat. Neurosci.* **8,** 346–353

11. Iwanami, A., Kaneko, S., Nakamura, M., Kanemura, Y., Mori, H., Kobayashi, S., Yamasaki, M., Momoshima, S., Ishii, H., Ando, K., et al. (2005) Transplantation of human neural stem cells for spinal cord injury in primates. *J. Neurosci. Res.* **80,** 182–190

12. Lewin, M., Carlesso, N., Tung, C. H., Tang, X. W., Cory, D., Scadden, D. T., and Weissleder, R. (2000) Tat peptide-derivatized magnetic nanoparticles allow in vivo tracking and recovery of progenitor cells. *Nat. Biotechnol.* **18,** 410–414

13. Bulte, J. W., Duncan, I. D., and Frank, J. A. (2002) In vivo magnetic resonance tracking of magnetically labeled cells after transplantation. *J. Cereb. Blood Flow Metab.* **22,** 899–907

14. Graves, E. E., Weissleder, R., and Ntziachristos, V. (2004) Fluorescence molecular imaging of small animal tumor models. *Curr. Mol. Med.* **4,** 419–430

15. Jendelova, P., Herynek, V., Urdzikova, L., Glogarova, K., Kroupova, J., Andersson, B., Bryja, V., Burian, M., Hajek, M., and Sykova, E. (2004) Magnetic resonance tracking of transplanted bone marrow and embryonic stem cells labeled by iron oxide nanoparticles in rat brain and spinal cord. *J. Neurosci. Res.* **76,** 232–243

16. Lee, I. H., Bulte, J. W., Schweinhardt, P., Douglas, T., Trifunovski, A., Hofstetter, C., Olson, L., and Spenger, C. (2004) In vivo magnetic resonance tracking of olfactory ensheathing glia grafted into the rat spinal cord. *Exp. Neurol.* **187,** 509–516

17. Pirko, I., Johnson, A., Ciric, B., Gamez, J., Macura, S. I., Pease, L. R., and Rodriguez, M. (2004) In vivo magnetic resonance imaging of immune cells in the central nervous system with superparamagnetic antibodies. *FASEB J.* **18,** 179–182

18. Contag, C. H., and Bachmann, M. H. (2002) Advances in in vivo bioluminescence imaging of gene expression. *Annu. Rev. Biomed. Eng.* **4,** 235–260

19. Costa, G. L., Sandora, M. R., Nakajima, A., Nguyen, E. V., Taylor-Edwards, C., Slavin, A. J., Contag, C. H., Fathman, C. G., and Benson, J. M. (2001) Adoptive immunotherapy of experimental autoimmune encephalomyelitis via T cell delivery of the IL-12 p40 subunit. *J. Immunol.* **167,** 2379–2387

20. Mandl, S., Schimmelpfennig, C., Edinger, M., Negrin, R. S., and Contag, C. H. (2002) Understanding immune cell trafficking patterns via in vivo bioluminescence imaging. *J. Cell. Biochem. Suppl.* **39,** 239–248

21. Wang, X., Rosol, M., Ge, S., Peterson, D., McNamara, G., Pollack, H., Kohn, D. B., Nelson, M. D., and Crooks, G. M. (2003) Dynamic tracking of human hematopoietic stem cell engraftment using in vivo bioluminescence imaging. *Blood* **102,** 3478–3482

22. Cao, Y. A., Wagers, A. J., Beilhack, A., Dusich, J., Bachmann, M. H., Negrin, R. S., Weissman, I. L., and Contag, C. H. (2004) Shifting foci of hematopoiesis during reconstitution from single stem cells. *Proc. Natl. Acad. Sci. USA* **101,** 221–226

23. Sweeney, T. J., Mailander, V., Tucker, A. A., Olomu, A. B., Zhang, W., Cao, Y., Negrin, R. S., and Contag, C. H. (1999) Visualizing the kinetics of tumor-cell clearance in living animals. *Proc. Natl. Acad. Sci. USA* **96,** 12,044–12,049

24. Miyoshi, H., Blomer, U., Takahashi, M., Gage, F. H., and Verma, I. M. (1998) Development of a self-inactivating lentivirus vector. *J. Virol.* **72,** 8150–8157

25. De, A., Lewis, X. Z., and Gambhir, S. S. (2003) Noninvasive imaging of lentiviral-mediated reporter gene expression in living mice. *Mol. Ther.* **7,** 681–691

26. Bai, Y., Soda, Y., Izawa, K., Tanabe, T., Kang, X., Tojo, A., Hoshino, H., Miyoshi, H., Asano, S., and Tani, K. (2003) Effective transduction and stable transgene expression in human blood cells by a third-generation lentiviral vector. *Gene Ther.* **10,** 1446–1457

27. Nagai, T., Ibata, K., Park, E. S., Kubota, M., Mikoshiba, K., and Miyawaki, A. (2002) A variant of yellow fluorescent protein with fast and efficient maturation for cell-biological applications. *Nat. Biotechnol.* **20,** 87–90

28. Scheff, S. W., Rabchevsky, A. G., Fugaccia, I., Main, J. A., and Lumpp, J. E., Jr. (2003) Experimental modeling of spinal cord injury: characterization of a force-defined injury device. *J. Neurotrauma* **20,** 179–193

29. Basso, D. M., Beattie, M. S., and Bresnahan, J. C. (1996) Graded histological and locomotor outcomes after spinal cord contusion using the NYU weight-drop device versus transection. *Exp. Neurol.* **139,** 244–256

30. Okada, S., Nakamura, M., Mikami, Y., Shimazaki, T., Mihara, M., Ohsugi, Y., Iwamoto, Y., Yoshizaki, K., Kishimoto, T., Toyama, Y., et al. (2004) Blockade of interleukin-6 receptor suppresses reactive astrogliosis and ameliorates functional recovery in experimental spinal cord injury. *J. Neurosci. Res.* **76,** 265–276

31. Rice, B. W., Cable, M. D., and Nelson, M. B. (2001) In vivo imaging of light-emitting probes. *J. Biomed. Opt.* **6,** 432–440

32. Lendahl, U., Zimmerman, L. B., and McKay, R. D. (1990) CNS stem cells express a new class of intermediate filament protein. *Cell* **60,** 585–595

33. Ma, M., Basso, D. M., Walters, P., Stokes, B. T., and Jakeman, L. B. (2001) Behavioral and histological outcomes following graded spinal cord contusion injury in the C57Bl/6 mouse. *Exp. Neurol.* **169,** 239–254

34. Iwanami, A., Yamane, J., Katoh, H., Nakamura, M., Momoshima, S., Ishii, H., Tanioka, Y., Tamaoki, N., Nomura, T., Toyama, Y., et al. (2005) Establishment of graded spinal cord injury model in a nonhuman primate: The common marmoset. *J. Neurosci. Res.* **80,** 172–181

35. Naldini, L., Blomer, U., Gallay, P., Ory, D., Mulligan, R., Gage, F. H., Verma, I. M., and Trono, D. (1996) In vivo gene delivery and stable transduction of nondividing cells by a lentiviral vector. *Science* **272,** 263–267

36. Tang, Y., Shah, K., Messerli, S. M., Snyder, E., Breakefield, X., and Weissleder, R. (2003) In vivo tracking of neural progenitor cell migration to glioblastomas. *Hum. Gene Ther.* **14,** 1247–1254

37. Kim, D. E., Schellingerhout, D., Ishii, K., Shah, K., and Weissleder, R. (2004) Imaging of stem cell recruitment to ischemic infarcts in a murine model. *Stroke* **35,** 952–957

38. Shah, K., Tang, Y., Breakefield, X., and Weissleder, R. (2003) Real-time imaging of TRAIL-induced apoptosis of glioma tumors in vivo. *Oncogene* **22,** 6865–6872

39. Coumans, J. V., Lin, T. T., Dai, H. N., MacArthur, L., McAtee, M., Nash, C., and Bregman, B. S. (2001) Axonal regeneration and functional recovery after complete spinal cord transection in rats by delayed treatment with transplants and neurotrophins. *J. Neurosci.* **21,** 9334–9344

40. Nakamura, M., Houghtling, R. A., MacArthur, L., Bayer, B. M., and Bregman, B. S. (2003) Differences in cytokine gene expression profile between acute and secondary injury in adult rat spinal cord. *Exp. Neurol.* **184,** 313–325

41. Bonni, A., Sun, Y., Nadal-Vicens, M., Bhatt, A., Frank, D. A., Rozovsky, I., Stahl, N., Yancopoulos, G. D., and Greenberg, M. E. (1997) Regulation of gliogenesis in the central nervous system by the JAK-STAT signaling pathway. *Science* **278,** 477–483

42. Nakashima, K., Yanagisawa, M., Arakawa, H., Kimura, N., Hisatsune, T., Kawabata, M., Miyazono, K., and Taga, T. (1999) Synergistic signaling in fetal brain by STAT3-Smad1 complex bridged by p300. *Science* **284,** 479–482

43. Llado, J., Haenggeli, C., Maragakis, N. J., Snyder, E. Y., and Rothstein, J. D. (2004) Neural stem cells protect against glutamate-induced excitotoxicity and promote survival of injured motor neurons through the secretion of neurotrophic factors. *Mol. Cell. Neurosci.* **27,** 322–331

Received April 13, 2005; accepted July 15, 2005.

Table 1

The percentages of differentiated cell types derived from the donor cells in vivo[a]

	GFAP	APC	Hu
Acute TP	80.7 ± 3.7	0.99 ± 0.4	1.27 ± 0.5
Delayed TP	61.0 ± 6.1	8.33 ± 1.1	11.8 ± 1.2

[a]The percentage of Hu/GFP double-positive neurons or APC/GFP double-positive oligodendrocytes among the GFP positive cells was ten times greater in the delayed transplantation (TP) group than that of the acute transplantation group.

Fig. 1

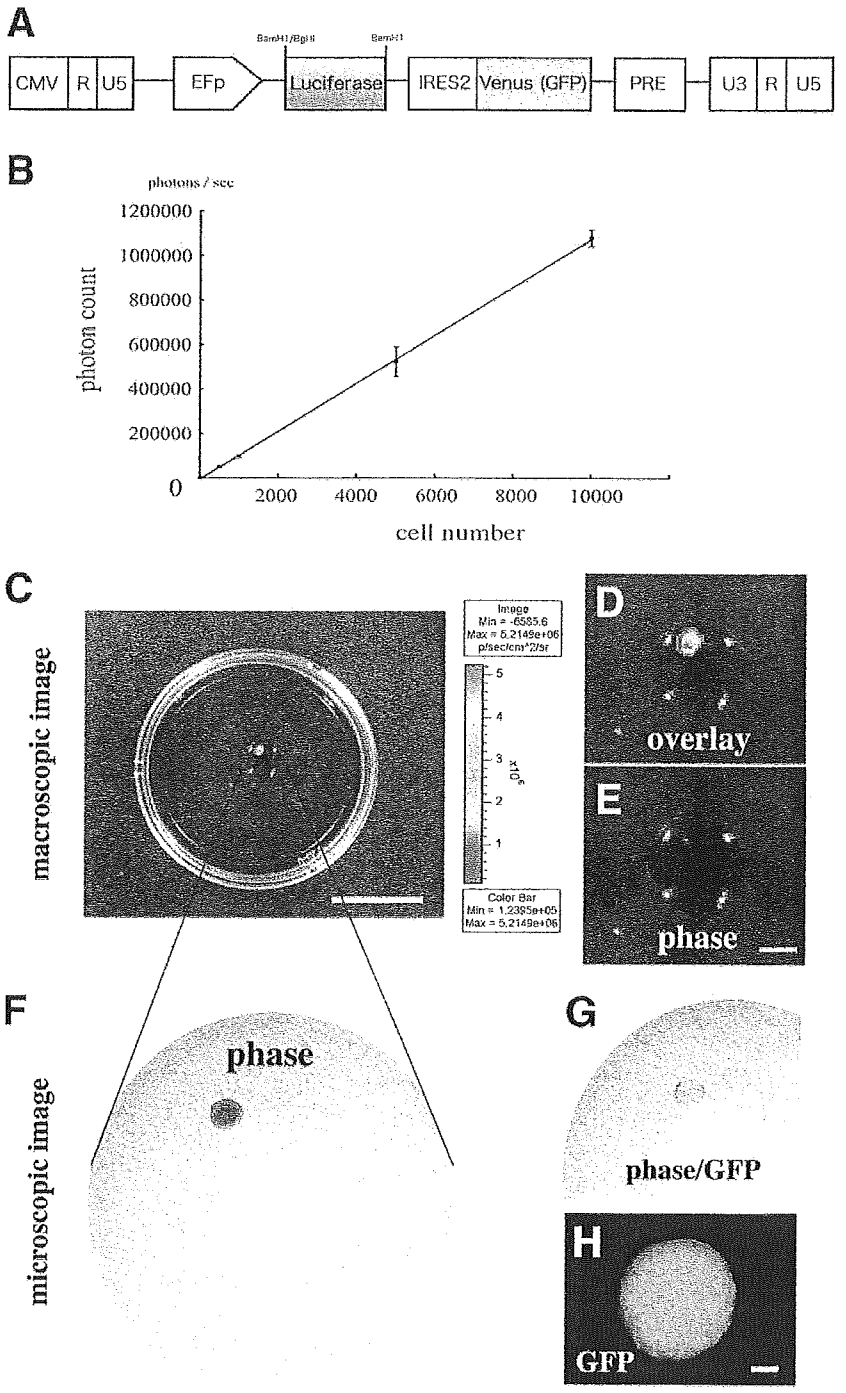

Figure 1. Sufficient expression of luminescence and fluorescence in the lentivirally transfected NSPCs. ***A)*** Lentiviral construct encoding a dual function luciferase and GFP bicistronic reporter gene connected via an internal ribosomal entry site (IRES). ***B)*** The correlation between photon counts and numbers of NSPCs expressing luciferase transduced by lentivirus. ***C–H)*** Macroscopic and microscopic images of a single neurosphere of transfected NSPCs in a drop of the medium. A single neurosphere expressed sufficient luminescence as well as fluorescence to be detected by the CCD macroscope or fluorescent microscope. Values are means ± SE (n=8). Scale bar: 15 mm (***C***), 2 mm (***E***), and 50 μm (***H***).

Fig. 2

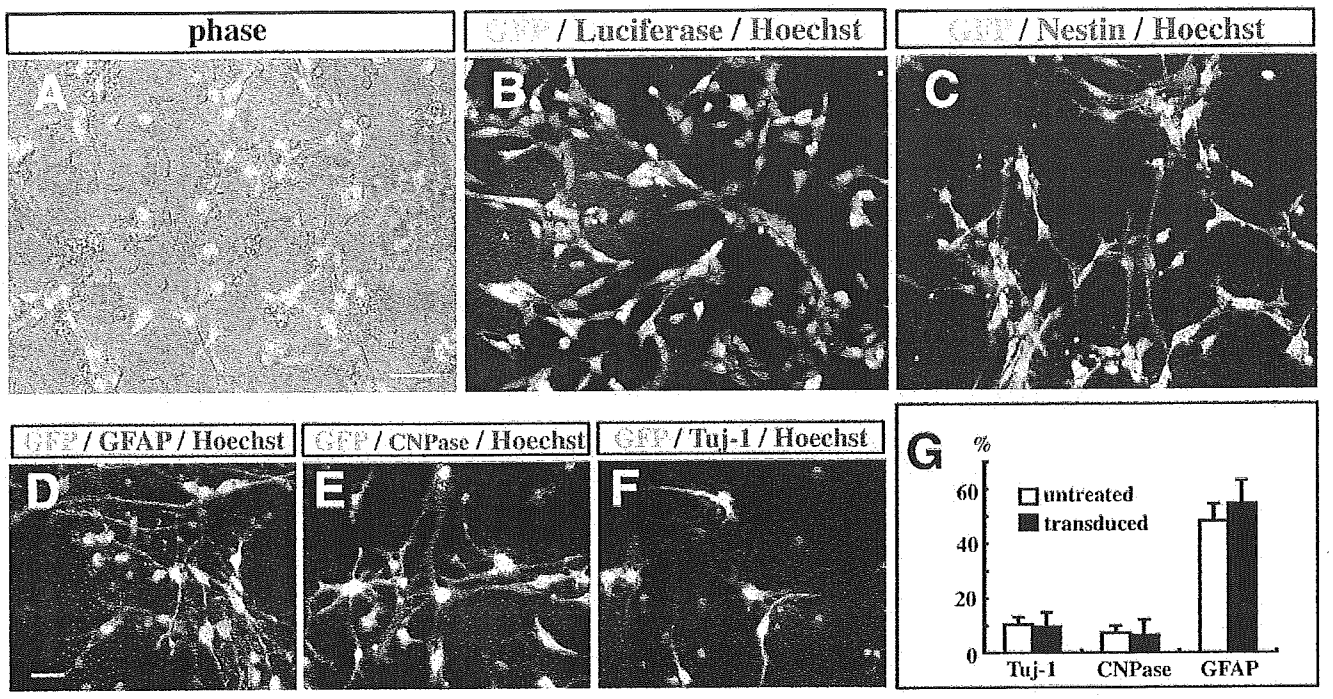

Figure 2. Lentiviral transduction did not influence the character of NSPCs. ***A, B***) Fluorescence microscopy and immunostaining with anti-luciferase antibody confirmed the expression of GFP and luciferase after differentiation. Immunohistochemistry showed that derivatives of NSPCs were reactive for nestin (***C***), GFAP (***D***), CNPase (***E***), and Tuj-1 (***F***). ***G***) The proportion of differentiated phenotypes in the lentivirally transduced NSPCs was identical to that of untreated NSPCs. Values are means ± SE (n=3). Scale bar: 50 μm (***A***) and 25 μm (***D***).

Fig. 3

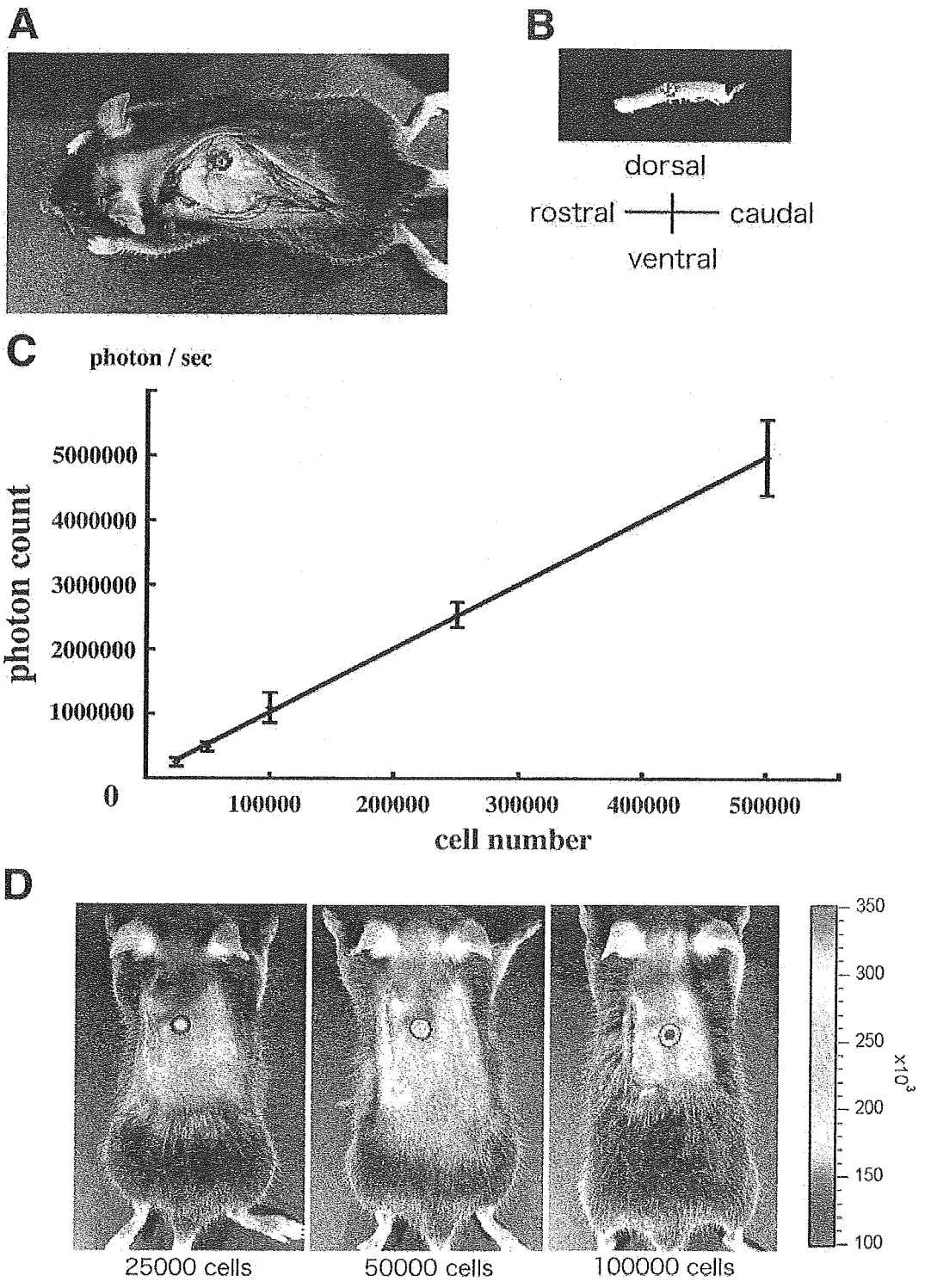

Figure 3. In vivo and ex vivo images of transplanted luciferase-expressing NSPCs into the intact spinal cord of mice. Accurate transplantation into spinal cord without leaking could be confirmed by the in vivo images (***A***) and ex vivo images (***B***) of exposed spinal cord. ***C, D)*** The correlation between grafted cell numbers and luminescent intensity was also confirmed in vivo. Values are means ± SE (n=4).

Fig. 4

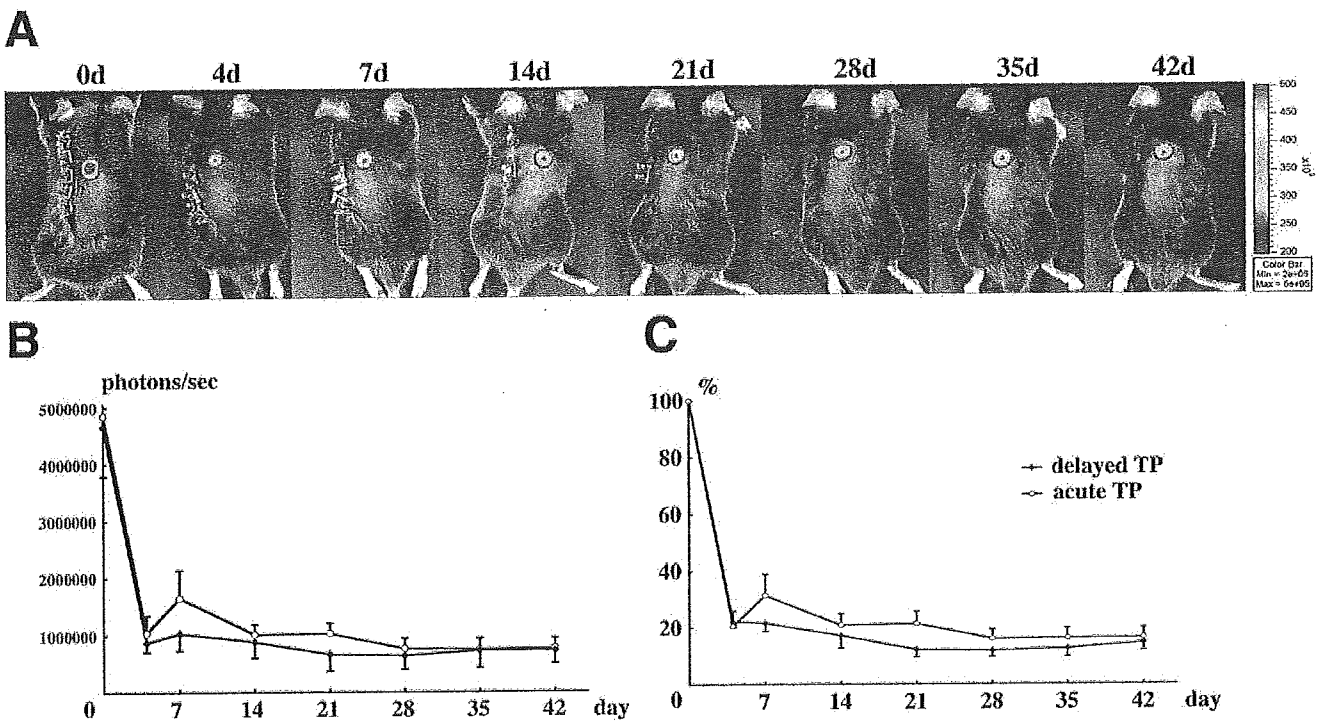

Figure 4. The time course of viability of transplanted NSPCs for SCI. ***A***) Images of a representative mouse that received acute transplantation (TP) of luciferase-expressing NSPCs confirmed long-term cell viability. Drastic reductions in signal intensity within the first 4 days after transplantation and then relatively stable bioluminescent signals for the following 6 wk were observed in both acute and delayed transplantation groups. There were no differences between acute and delayed transplantation groups in both value of signal intensity (***B***) and the rate to initial value (***C***) at each time point. Values are means ± SE (n=8).

Fig. 5

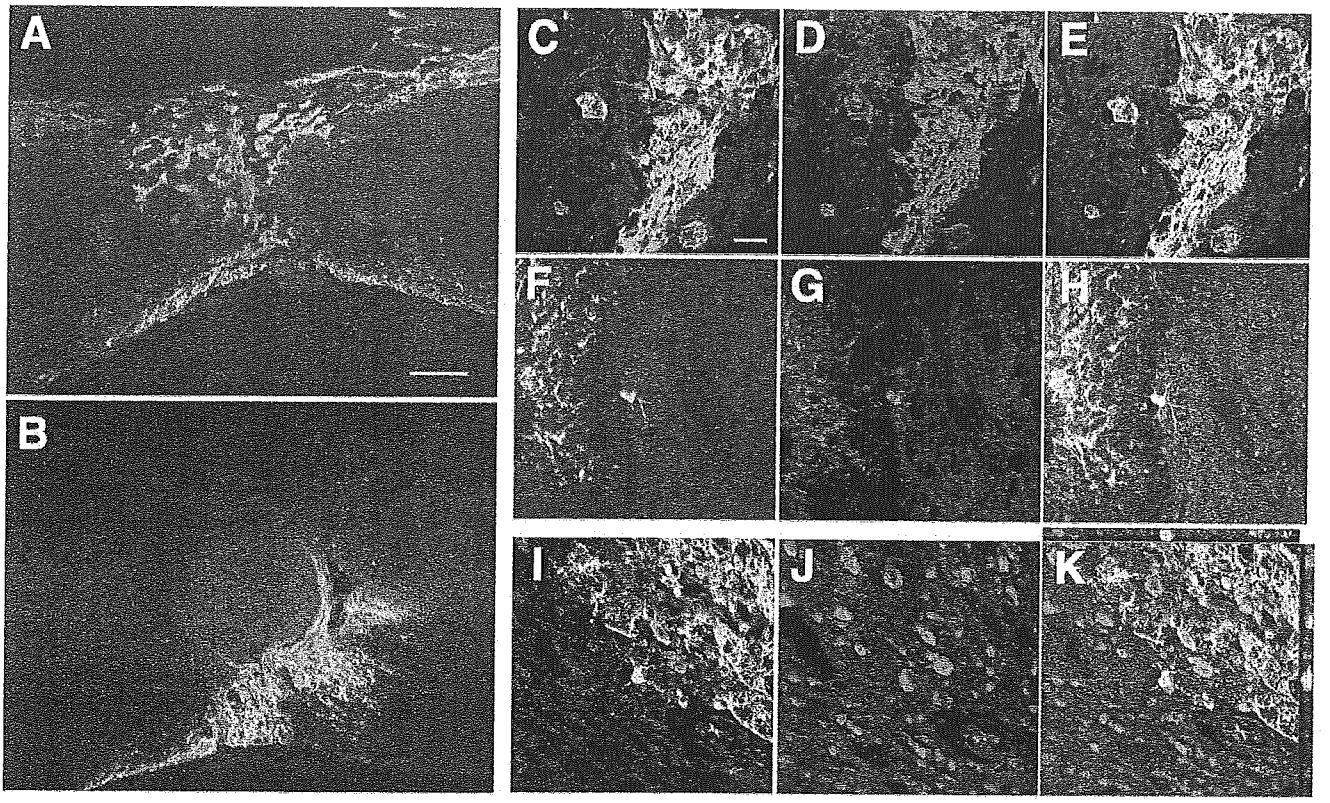

Figure 5. Transplanted NSPCs integrated and differentiated in the injured spinal cord at 6 wk after injury. Integrated cells were morphologically different between acute (***A***, ***C–E***) and delayed (***B***, ***F–K***) transplantation groups. A majority of transplanted NSPCs in the acute phase were immunoreactive for GFAP (***C–E***) and formed a glial scar at the lesion epicenter. In contrast, delayed transplanted NSPCs integrated around the scar tissue area, and a portion of these cells were identified as single cells differentiated into APC-positive oligodendrocytes with multiple myelin-forming processes (***F–H***) or Hu-positive neurons (***I–K***). Green represents GFP-positive NSPCs, and blue (***H***) represents Hoechst. ***K***) Orthogonal view to confirm the double labeling with Hu and GFP. Scale bar: 200 μm (***A***) and 25 μm (***C***).

Fig. 6

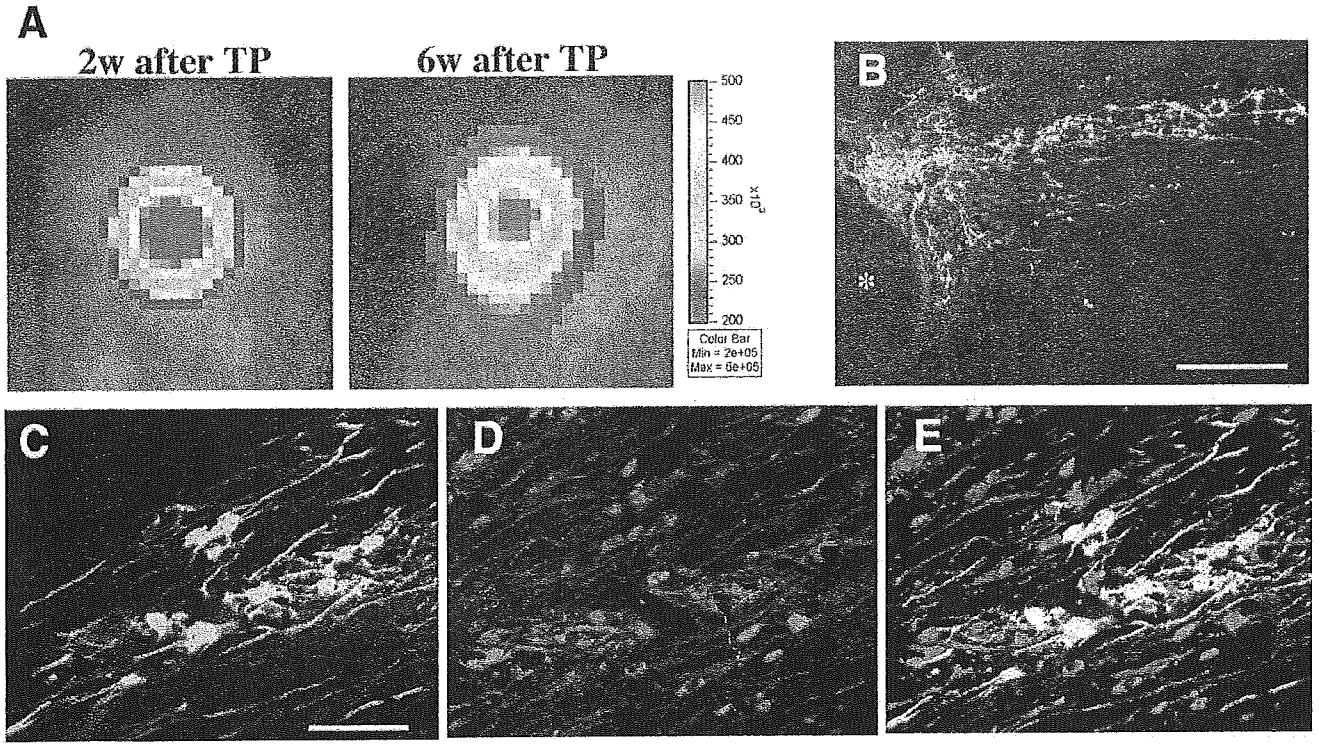

Figure 6. Representative image of configuration shift in BLI and histology of migratory cells in delayed transplantation group. ***A***) The signal configuration of grafted NSPCs, which was round at 2 wk after transplantation, became elliptical at 6 wk after transplantation. ***B***) Histological analysis revealed integrated cells migrating away from the scar area at lesion epicenter (*) in a caudal direction with extended neurites. The confocal image revealed that a portion of these cells were Hu-positive neurons (***C–E***). Scale bar: 200 μm (***B***) and 50 μm (***C***).

Fig. 7

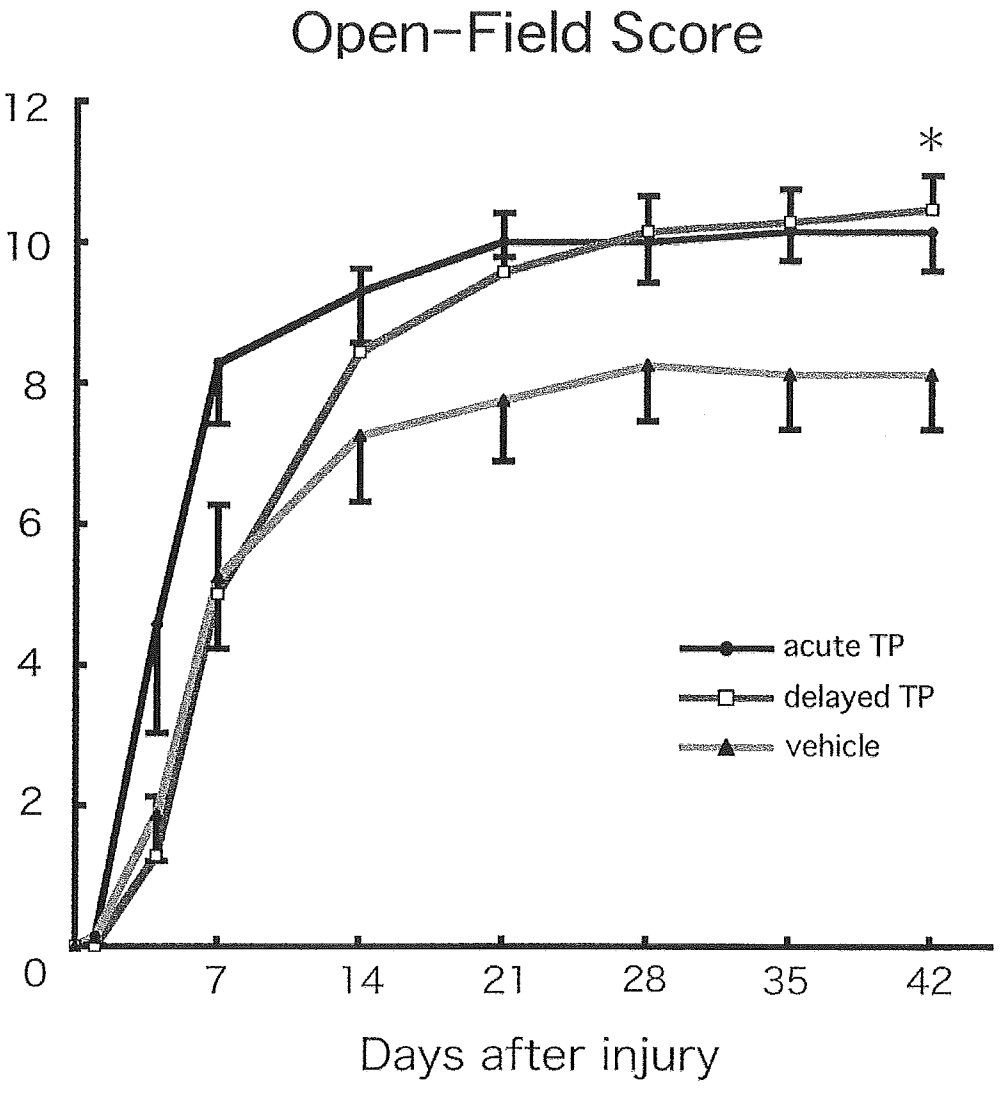

Figure 7. Partial functional recovery of paraplegic mice by transplantation of NSPCs. Both acute and delayed transplantation (TP) of NSPCs promoted recovery of hindlimb movement compared with vehicle injection (vehicle). There was a statistically significant difference between the delayed TP group and the vehicle-treated group in BBB score at 6 wk after injury. Values are means ± SE (n=8); *$P < 0.05$.

STEM CELLS®
Rapid Communication

Comparison of Various Bone Marrow Fractions in the Ability to Participate in Vascular Remodeling After Mechanical Injury

MAKOTO SAHARA,[a] MASATAKA SATA,[a,b,d] YUMI MATSUZAKI,[c,e] KIMIE TANAKA,[a] TOSHIHIRO MORITA,[a] YASUNOBU HIRATA,[a] HIDEYUKI OKANO,[c,e] RYOZO NAGAI[a]

Departments of [a]Cardiovascular Medicine and [b]Advanced Clinical Science and Therapeutics, University of Tokyo Graduate School of Medicine, Tokyo, Japan; [c]Department of Physiology, Keio University School of Medicine, Tokyo, Japan; [d]PRESTO, Japan Science and Technology Agency, Kawaguchi, Saitama, Japan; [e]CREST, Japan Science and Technology Agency, Kawaguchi, Saitama, Japan

Key Words. Endothelial cells • Hematopoietic stem cells • Progenitor • Smooth muscle cells • Transdifferentiation

ABSTRACT

In contrast to conventional assumption, recent reports propose the possibility that hematopoietic stem cells (HSCs) may have broader potential to differentiate into various cell types. Here, we tested the pluripotency of HSCs by comparing vascular lesions induced by mechanical injury after bone marrow reconstitution with total bone marrow (TBM) cells, c-Kit$^+$ Sca-1$^+$ Lin$^-$ (KSL) cells, or a single HSC cell (Tip-SP CD34$^-$ KSL cell, CD34$^-$ c-Kit$^+$ Sca-1$^+$ Lin$^-$ cell with the strongest dye-efflux activity) harboring green fluorescent protein (GFP). The lesions contained a significant number of GFP-positive cells in the TBM and KSL groups, whereas GFP-positive cells were rarely detected in the HSC group. These results suggest that transdifferentiation of a highly purified HSC seems to be a rare event, if it occurs at all, whereas bone marrow cells including the KSL fraction can give rise to vascular cells that substantially contribute to repair or lesion formation after mechanical injury. STEM CELLS *2005;23:874–878*

INTRODUCTION

Recent evidence suggests that bone marrow–derived cells may participate in regeneration of remote organs [1]. Bone marrow contains both hematopoietic and nonhematopoietic cells. Hematopoietic stem cells (HSCs) are defined as having the capacity for self-renewal and the ability to differentiate into all mature hematopoietic lineages [2]. Although it was assumed that HSCs give rise to hematopoietic cells, recent reports proposed the possibility that HSCs may have the broader potential to differentiate into nonhematopoietic cells, including epithelial cells [3], hepatocytes [4, 5], cardiomyocytes [6], and vascular cells [7]. In contrast, others cast doubt on the pluripotency of adult HSCs under physiological conditions by analyzing uninjured organs of bone marrow chimeric mice [8].

There might be two possibilities that account for the discrepancy. First, the HSCs used differ in their purity [4, 7, 8]. Most of the studies analyzed the CD34$^-$, c-Kit$^+$, Sca-1$^+$, Lineage$^-$ (CD34$^-$KSL) bone marrow cells [4, 7], which have been assumed as the most primitive HSCs [9]. However, even in the best case series reported [9], only one in five recipients showed successful engraftment after single-cell transplantation, indicating that the CD34$^-$KSL fraction represents a heterogeneous population containing nonhematopoietic cells. It is possible that nonhematopoietic cells among the CD34$^-$KSL cells might be responsible for the pluripotency. Second, the apparent discrepancy could merely derive from the analysis of noninjured versus injured tissues [10]. We reported that the mode of injury is crucial for the recruitment

Correspondence: Masataka Sata, M.D., Department of Cardiovascular Medicine, University of Tokyo Graduate School of Medicine, 7-3-1 Hongo, Bunkyo-ku, Tokyo 113-8655, Japan. Telephone: 81-3-3815-5411; Fax: 81-3-3814-0021; e-mail: msata-circ@umin.ac.jp Received January 11, 2005; accepted for publication May 19, 2005; first published online in STEM CELLS *EXPRESS* June 7, 2005.
1066-5099/2005/$12.00/0 doi: 10.1634/stemcells.2005-0012

of bone marrow–derived cells to vascular remodeling [11]. Thus, it remains unclear whether a highly purified single HSC can contribute to vascular remodeling after severe vascular injuries, which are essential for bone marrow–derived cells to participate in vascular remodeling.

Here, we transplanted either total bone marrow (TBM) cells, KSL fraction cells, or a highly purified HSC into lethally irradiated wild-type mice [2]. In all groups, peripheral blood cells were successfully reconstituted. However, bone marrow–derived cells were seldom detected in the injured artery when a single HSC was injected into irradiated mice. These results suggest that it is a rare property for a purified HSC to transdifferentiate into vascular cells.

Materials and Methods

Animals

All wild-type mice were purchased from SLC (Shizuoka, Japan). Transgenic mice (C57BL/6 background) that ubiquitously express enhanced green fluorescent protein (GFP) were described in previous reports [2, 7]. All procedures involving experimental animals were performed in accordance with protocols approved by the institutional committee for animal research of the University of Tokyo and complied with National Institutes of Health guidelines.

Preparation of TBM Cells, KSL Cells, and a Highly Purified HSC

TBM cells were harvested from femora and tibias of the GFP-transgenic mice as previously described [7]. c-Kit$^+$, Sca-1$^+$, Lineage$^-$ fraction of bone marrow cells (KSL cells) were purified as described [7]. Briefly, TBM cells were stained with a cocktail of biotinylated monoclonal antibodies against lineage markers (B220/CD45R, clone RA3-6B2; Mac-1, clone M1/70; Gr-1, clone RB6-8C5; Thy1.2, clone 53-2.1; CD3, clone 145-2C11; CD4, clone GK1.5; CD8, clone 53-6.72; and TER 119, clone Ly-76; Pharmingen, San Diego, http://www.bdbiosciences.com/pharmingen) for 20 minutes at 4°C. The cells were treated with streptavidin-conjugated immunomagnetic beads (BioMag; Polysciences, Inc., Warrington, PA, http://www.polysciences.com/shop) for 30 minutes to remove highly lineage-positive cells. The remaining cells were collected and stained with a phycoerythrin (PE)–conjugated anti–Sca-1 antibody (Pharmingen), an allophycocyanin-conjugated anti–c-Kit antibody (Pharmingen), and PE Texas red–conjugated streptavidin (Pharmingen) for 20 minutes at 4°C. KSL cells were purified by fluorescence-activated cell sorting (ALTRA; Beckman-Coulter, Tokyo, http://www.beckmancoulter.com). The bone marrow cells that had the strongest dye-efflux activity (Tip–side population [SP] cells) with a phenotype of CD34$^-$ c-Kit$^+$ Sca-1$^+$ Lineage$^-$ (CD34$^-$KSL) were isolated as described [2]. A single-cell transplantation analysis has revealed that the Tip-SP CD34$^-$KSL cells represent the most primitive hematopoietic stem cells, with nearly complete hematopoietic engraftment activity [2].

Stem Cell Transplantation

After lethal irradiation of 10.5 Gy (MBR-1520RB; Hitachi, Tokyo, http://www.hitachi.com), 1×10^6 TBM cells (TBM group), 3×10^3 KSL cells (KSL group), or a single Tip-SP CD34$^-$KSL cell (HSC group) from GFP-transgenic mice were suspended in 0.3 ml phosphate-buffered saline and injected intravenously by tail vein puncture into C57BL/6 mice. The sites of intravenous injection, that is, tail vein or retro-orbital plexus, had no effect on the level of reconstitution (Y. Matsuzaki and H. Nakauchi, unpublished observations). The single Tip-SP CD34$^-$KSL cell was transplanted with 2×10^5 TBM cells from C57BL/6 mice for radioprotection. Eight to 16 weeks after transplantation, peripheral blood samples were collected from the retro-orbital venous plexus. After erythrocytes were lysed with ACK lysing buffer (0.155 M ammonium chloride, 0.1 M disodium EDTA, and 0.01 M potassium bicarbonate) [12], cell suspensions were analyzed by flow cytometry to measure GFP signal (XL; Beckman-Coulter).

Wire-Mediated Endovascular Injury and Histological Analysis

At 12 weeks after irradiation and stem cell transplantation, an endovascular arterial injury was induced to the femoral artery of the bone marrow chimeric mice by inserting a large wire (0.38 mm in diameter, No. C-SF-15-15 [Cook, Bloomington, IN, http://www.cookgroup.com/profile/med-mfg/index.html]) as described [7, 11, 13]. At 4 weeks, the injured femoral arteries were excised and fixed in 4% paraformaldehyde. To preserve GFP signal for histological analyses, the arteries were embedded in plastic resin (Technovit 8100; Heraeus Kulzer, Wehrheim, Germany, http://www.heraeus-kulzer-us.com) as described. Immunofluorescence double staining was performed as described elsewhere [7]. The plastic-embedded sections were incubated with primary antibodies (Cy3-conjugated anti–α-smooth muscle actin [α-SMA], clone 1A4 [Sigma, St. Louis, http://www.sigmaaldrich.com]; anti-CD31, clone MEC13.3 [BD Biosciences, San Jose, CA, http://www.bdbiosciences.com/index.shtml]; anti–pan-endothelial cell antigen, clone MECA-32 [BD Biosciences]; anti-CD45, clone 30-F11 [BD Biosciences]) followed by incubation with Cy3-conjugated secondary antibodies (Jackson ImmunoResearch, West Grove, PA, http://www.jacksonimmuno.com). Nuclei were counterstained with Hoechst 33258 (Sigma). The sections were mounted with the ProLong Antifade Kit (Molecular Probes, Eugene, OR, http://probes.invitrogen.com) and observed under confocal microscopes (FLUOVIEW FV300; Olympus, Tokyo, http://www.olympus-global.com/en/global). Cell number was counted in the neointima and media of a cross-section of each artery [7, 11]. Frequency of GFP-positive cells among total cells is reported.